Neutron Spin−Echo Study of the Dynamic Behavior of Amphiphilic Diblock Copolymer Micelles in Aqueous Solution

Hideki Matsuoka, Yusuke Yamamoto, Minoru Nakano, Hitoshi Endo, and Hitoshi Yamaoka*,†

Department of Polymer Chemistry, Kyoto University, Kyoto 606-8501, Japan

Reiner Zorn, Michael Monkenbusch, and Dieter Richter

Institute für Festkörperforschungs, Forschungszentrum Jülich GmbH, D-52425 Jülich, Germany

Hideki Seto and Youhei Kawabata

FIAS, Hiroshima University, Higashi-Hiroshima, Hiroshima 739-8521, Japan

Michihiro Nagao

Neutron Scattering Laboratory, Institute of Solid State Physics, The University of Tokyo, Tokai, Ibaraki 319-1106, Japan

Received November 29, 1999. In Final Form: September 5, 2000

We examined the dynamics of amphiphilic polymer micelles of the diblock copolymer HOVE-NBVE (hydroxyethylvinyl ether as a hydrophilic segment and *n*-butylvinyl ether as a hydrophobic segment) in aqueous solution using the neutron spin−echo (NSE) technique. The time-correlation function obtained for the polymer micelles was well fitted by double exponential function, and the fast and slow modes could be estimated separately. The slow mode was dominant at smaller scattering angles, and showed an excellent linearity in Γ(decay rate) vs q^2 (scattering vector) plot. The diffusion coefficient evaluated from its slope and the hydrodynamic radius, R_h, by the Einstein−Stoke equation were consistent with the size of the polymer micelle that was estimated by small-angle neutron scattering (SANS), small-angle X-ray scattering (SAXS), and dynamic light scattering (DLS). Hence, this slow mode reflects the translational diffusion of the polymer micelle in aqueous solution. The fast mode, which was 1 order of magnitude faster than the slow mode, was a major factor for larger scattering angle regions in which the SANS curve showed blob scattering. Thus, the fast mode appears to be an internal motion of the polymer micelle, like the breathing mode of the hydrophilic shell (corona) around the polymer micelle.

1. Introduction

Amphiphilic polymers, sometimes called polymer surfactants, are a class of macromolecules that consist of hydrophobic and hydrophilic segments connected by a covalent bond. The coexistence of these two kinds of segments in a single polymer chain is expected to produce very interesting characteristics, such as surface activity, and micellization. In the 1950s,[1] the possibility of micelle formation by block copolymers in selective solvents was pointed out, and in 1964, Krause discovered micelle formation in fractionated samples of a methyl methacrylate-styrene-methyl methacrylate triblock copolymer in solution by systematic light scattering (LS) and viscosity measurements.[2] A larger molecular weight characteristic of micelles was obtained by LS both for solutions in acetone (a nonsolvent for polystyrene) and triethylbenzene (a nonsolvent for polymethymethacrylate). More recently, micelle formation by di- and triblock copolymers in selective solvents has been reported.[3−10] Recently, it has become possible to synthesize diblock copolymers whose segment length is precisely controlled by living cationic polymerization[11] by the development of synthetic techniques, which give us quantitative information on the micellization mechanism. However, most of the previous polymer micelle studies were for organic solvent systems, and aqueous studies had been limited to so-called Pluronic systems, such as poly(ethylene oxide)(PEO)/poly(propylene oxide) (PPO) and PEO/poly(butylene oxide) (PBO), which are commercially available. A few investigators have reported studies on the micellization for other aqueous

* To whom correspondence should be addressed.

† Present address: Department of Materials Science, University of Shiga Prefecture, Hassaka-cho, Hikone, Shiga 522-8533, Japan.

(1) Marrett, E. M. *J. Polym. Sci*. **1967**, *24*, 467.

(2) Krause, S. *J. Phys. Chem*. **1964**, *68*, 1948.

(3) Riess, G. In *Encyclopedia of Polymer Science and Engineering*; 2nd ed., John Wiley: NY, 1985; Vol. 2, p 324.

(4) Halperin, A.; Tirrel, M.; Lodge, T. P. *Adv. Polym. Sci*. **1992**, *100*, 31.

(5) Tuzar, Z.; Kratochvil, P. In *Surfaces and Colloid Science*; Matijevic', E., Ed.; Plenum Press: New York, 1993; Vol. 15, p 1.

(6) Hilfiker, R.; Chu, B.: Xu, Z. *J. Colloid Interface Sci*. **1989**, *133*, 176. Hilfiker, R.; Wu, D. Q.; Chu, B. *J. Colloid Interface Sci* **1990**, *135*, 573.

(7) Gao, Z.; Zhong, X.-F.; Eisenberg, A. *Polym. Prepr*. **1994**, *35*, 570.

(8) Antonetti, M.; Heintz, S.; Schmidt, M.; Rosenauer, C. *Macromolecules* **1994**, *27*, 3276.

(9) Munch, M. R.; Gast, A. P. *Macromolecules* **1988**, *21* 1360.

(10) Qin, A.; Tian, M.; Ramireddy, C.; Webber, S. E.; Munk, P.; Tuzar, Z. *Macromolecules* **1994**, *27*, 120.

(11) Minoda, M; Sawamoto, M; Higashimura, T. *Macromolecules* **1987**, *20*, 2045.

10.1021/la9915421 CCC: $19.00
Published on Web 11/03/2000

Table 1. Characteristics of Block Copolymer Used and Their Micelles in Aqueous Solution

	micelle size parameters by scattering techniques						
				$R_{g,Guinier}$			
sample (m:n)	R_s by SANS	R_c by SANS	N_{agg} by SANS	by SANS	by SAXS	R_h by DLS	R_{gGauss} by SANS
N496 (49:6)	66 Å (25 °C)	20 Å (25 °C)	32	49 Å (25 °C)	58 Å (25 °C)	68 Å (21 °C)	45 Å
($M_w/M_n = 1.07$)				48 Å (45 °C)		73 Å (44 °C)	
N338 (33:8)	70 Å (25 °C)	32 Å (25 °C)	98				35 Å
($M_w/M_n = 1.10$)							

[a] R_s, radius of shell + core; R_c, core radius; $R_{g,Guinier}$, radius of gyration by Guinier analysis; N_{agg}, aggregation number; R_h, hydrodynamic radius; R_{gGauss}, R_g for blob scattering.

solution systems.[12−14] However, in these few years, the number of studies on the aqueous system has increased very rapidly.

The importance of studying amphiphilic polymer micellization in aqueous systems is obvious if one takes the phenomena in biological systems into account. In fact, the number of studies on aqueous systems has recently increased and interesting phenomena have been found. For example, Nakano et al.[15] performed a systematic small-angle X-ray scattering (SAXS) and small-angle neutron scattering (SANS) study on diblock amphiphilic copolymers of vinyl ether in aqueous solution. They evaluated the whole shape and detailed internal structure of polymer micelles as a function of the hydrophobic chain length (i.e., hydrophobicity), and found a sphere-rod transition of micelle geometry. They observed the coexistence of rodlike micelles and spherical micelles. They also performed a systematic SAXS study for amphiphilic polymer micelles having an octadecyl chain as a hydrophobic segment as a function of solution temperature.[16] They found a disklike micelle at lower temperatures, whereas a spherical micelle was observed at higher temperature. These observations suggest that the melting temperature of the hydrophobic core has an important role in the morphology of polymer micelles. Various novel amphiphilic block copolymers containing silicon, fluorine, etc. have been synthesized and their association behavior, micellar structure and its transition, and unique characters such as specific solubilization of hydrophobic molecules, have been reported.[17−20]

As mentioned above, structural studies on micelle geometry in aqueous media are now being systematically performed by several researchers. Our next interest is the dynamics of micelle structure. For nonaqueous systems, studies have been performed by using the neutron spin−echo (NSE) technique. NSE was established by the pioneering work by Mezei.[21,22] NSE can detect quasielastic and inelastic scattering from the system, from which a dynamic character of the system can be evaluated. A famous example of the application of NSE to polymer systems is the important work by Richter et al.[23,24] who observed the reptation motion in polymer melts. Later, Farago et al.[25a,b] and Takeda et al.[25c] performed systematical and extensive NSE works on the deformation of microemulsion droplets. Because the NSE technique provides information on the dynamics in the length scale of polymers and polymer assemblies, this technique should be useful for studying the dynamics of polymer micelles. Dynamic light scattering (DLS) is now generally used to evaluate the dynamics in the system, but the dimension of the structure of the system is limited to a large region because of the limitation of q (the scattering vector: $q = 4\pi n \sin\theta/\lambda$, 2θ is the scattering angle, λ is the wavelength of neutron, X-ray, and laser light, n is the refractive index of the medium) range covered. In fact, some NSE studies on polymer micelles in nonaqueous media have been reported,[26] and NSE should be useful to examine the dynamics of the hydrophilic shell (corona) around the polymer micelle.

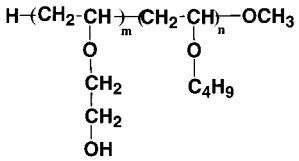

Figure 1. Structure of amphiphilic diblock copolymer used in this study.

Here, we performed a systematic NSE study for diblock copolymer micelles in aqueous solution to estimate the dynamic properties of this system.

2. Experimental Section

a. Samples. The polymer sample used was a diblock copolymer of hydroxyethylvinyl ether as a hydrophilic segment and *n*-butylvinyl ether as a hydrophobic segment (HOVE-NBVE). (Figure 1). We denote the degree of polymerization of hydrophilic and hydrophobic segments by m and n, respectively. Two samples, one with an m:n = 49:6 (N496) and another with that of 33:8 (N338) were used. The polydispersity index (M_w/M_n) by gel permeation chromatography before hydrolysis was 1.07 and 1.10, respectively. These copolymers were synthesized in our laboratory. Complete details of the procedure of synthesis appear elsewhere.[15] The characteristic properties of the polymers used are summarized in Table 1. The diblock copolymer synthesized was purified by dialysis against Milli-Q water and then lyo-

(12) Xu, R.; Winnik, M. A.; Hallett, F. R.; Riess, G.; Croucher, M. D. *Macromolecules* **1991**, *24*, 87.
(13) Zhu, J.; Lennox, B.; Eisenberg, A. *J. Phys. Chem.* **1992**, *96*, 4727.
(14) Kriz, J.; Plestil, J.; Tuzar, Z.; Pospisil, H.; Brusm J.; Jakes, J.: Masar, B.; Vlcek, P.; Doskocilova, D. *Macromolecules* **1999**, *32*, 397.
(15) Nakano, M.; Matsuoka, H.; Yamaoka, H.; Poppe, A.; Richter D. *Macromolecules* **1999**, *32*, 697.
(16) Nakano, M.; Matsumoto, K.: Matsuoka, H.; Yamaoka, H. *Macromolecules* **1999**, *32*, 4029.
(17) Matsumoto, K.; Miyagawa, K.; Matsuoka, H.; Yamaoka, H. *Polym. J.* **1999**, *31*, 609.
(18) Nakano, M.; Deguchi, M.; Matsumoto, K.; Matsuoka, H.; Yamaoka, H. *Macromolecules* **1999**, *32*, 7437.
(19) Nakano, M.; Deguchi, M.; Endo, H.; Matsumoto, K.; Matsuoka, H.; Yamaoka, H. *Macromolecules* **1999**, *32*, 6088.
(20) Matsumoto, K.; Kubota, M.; Matsuoka, H.; Yamaoka, H. *Macromolecules* **1999**, *32*, 7122.
(21) Mezei, F. *Z. Phys.* **1972**, *225*, 146.
(22) Mezei, F. *Neutron Spin−Echo*; Springer Verlag: NY, 1980. Ewen, B.; Richter, D. *Adv. Polym. Sci.* **1997**, *134*, 1.
(23) Richter, D.; Ewen, B.; Farago, B.; Wagner, T. *Phys. Rev. Lett.* **1989**, *62*, 2140.
(24) Richter, D.; Farago, B.; Fetters, L. J.; Huang, J. S.; Ewen, B.; Lartigue, C. *Phys. Rev. Lett.* **1990**, *64*, 1389.
(25) (a) Huang, J. S.; Milner, S. T.; Farago, B.; Richter, D. *Phys. Rev. Lett.* **1987**, *59*, 2600, (b) Farago, B.; Richter, D.; Huang, J. S.; Safran, S. A.; Milner, S. T. *Phys. Rev. Lett.* **1990**, *65*, 3348, (c) Takeda, T.; Komura, S.; Seto, H.; Nagai, M.; Kobayashi, H.; Yokoi, E.; Ebisawa, T.; Tasaki, S.; Zeyen, C. M. E.; Takahashi, S.; Yoshizawa, H. *Physica B* **1995**, *213&214*, 863. (d) Takeda, T.; Kawabata, Y.; Seto, H.; Ghosh, S. K.; Okuhara, D.; Komura, S.; Nagao, M.; Brulet, A.; Teixeira, J. *J. Phys. Chem. Sol.* **1999**, *60*, 1375.
(26) Farago, B.; Monkenbusch, M.; Richter, D.; Huang, J. S.; Fetters, L. J.; Gast, A. P. *Phys. Rev. Lett.* **1993**, *71*, 1015.

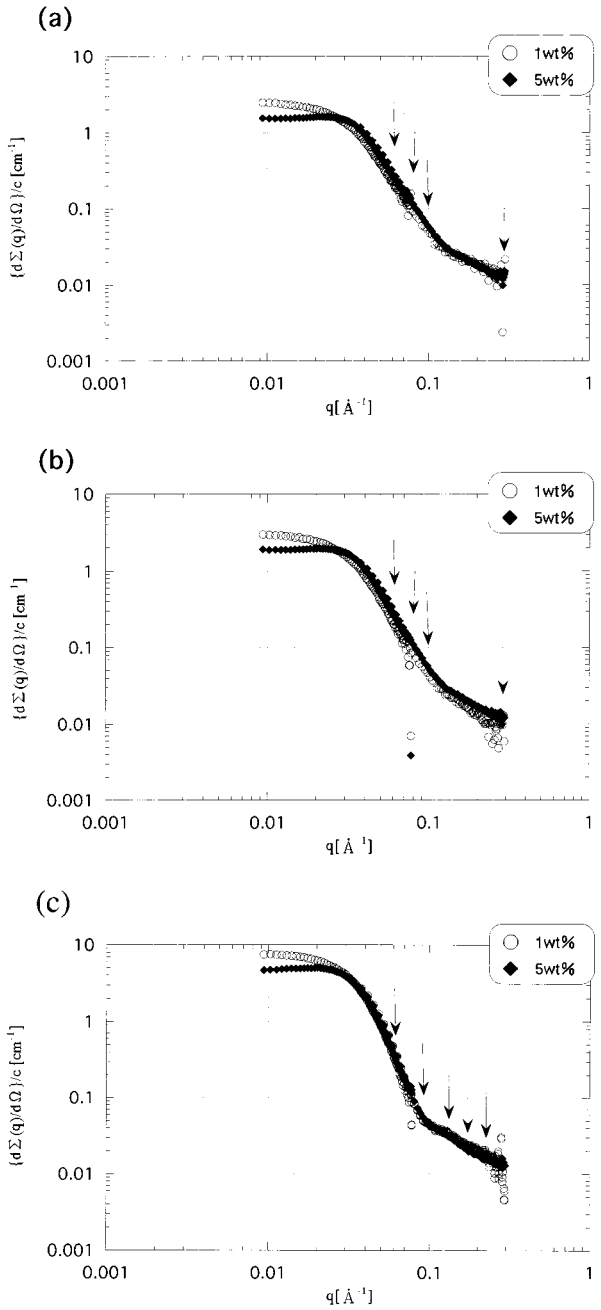

Figure 2. SANS profiles for N496 in 1 wt % and 5 wt % D_2O solutions at 21 °C (a) and 45 °C (b), and for N338 in 1 wt % and 5 wt % D_2O solutions at 25 °C (c).

philized. The solution samples were prepared by dissolving a suitable amount of polymer into deuterium hydroxide (Aldrich, D:99.98 at. %) as the solvent.

b. NSE Instruments and Experiments. NSE experiments for the N496 sample were performed using the NSE instrument at JRR-3M, Tokai, Japan which was constructed by Takeda et al. The details of this instrument have been fully described elsewhere.[25c,27] A specially designed quartz cell was used. The sample thickness was 5 mm. NSE experiments for N338 were performed at Forschungszentrum Jülich, Germany, for which details can be found elsewhere.[28] The sample solutions were put into a rectangular quartz cell. The accumulation time ranged from 6600 to 82 500 s depending on the sample and instrument. The temperature of the sample was controlled by circulating thermostated water for both instruments. Grafoil was used to measure the resolution function of the spectrometers.

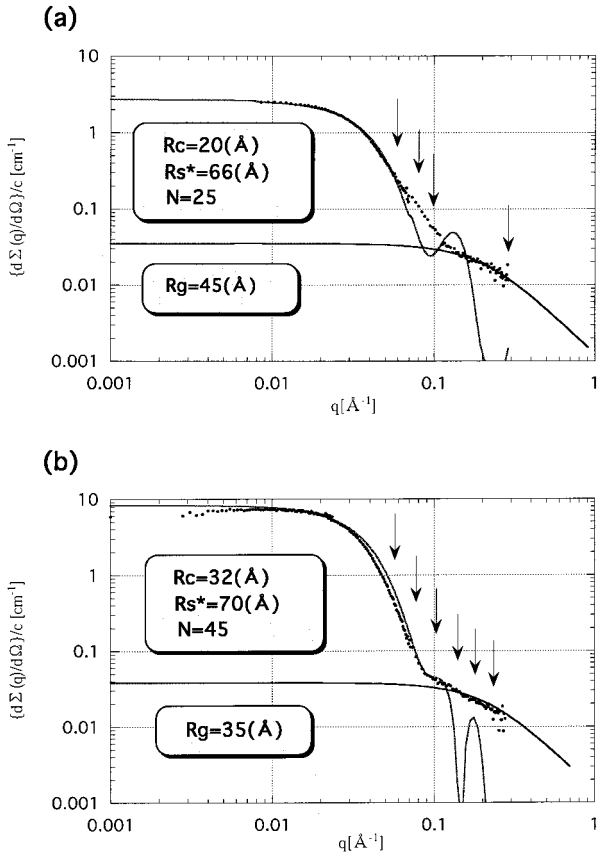

Figure 3. Model fitting of SANS profiles for N496 (a) and N338 (b) in 1 wt % D_2O solutions at 25 °C. The dots are the experimental data, the gray line (upper line in the small q region and with peak in large q region) was obtained by the core−shell spherical model. R_c is the core radius, R_s is the radius of core + shell, and N is the aggregation number (N_{agg} in Table 1). The black line (lower curve in the low q region which shows monotonical decrease) is the fitting curve for a higher q region ($q > 0.1$) by Debye function for the scattering from Gaussian coil. R_g is the radius of gyration of the coil (R_{gGauss} in Table 1).

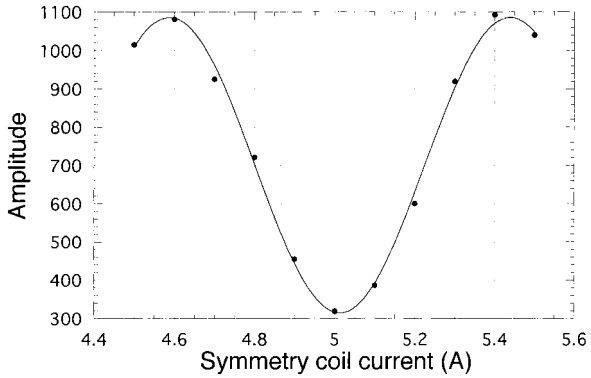

Figure 4. Typical example of echo signal at 21 °C for 5% N496; where q is 0.06 Å^{-1}.

c. SANS Experiments. To check the size and shape of the micelle in heavy water and also its change by temperature, the SANS measurements were performed using the SANS−U beam line of ISSP, University of Tokyo, at JRR-3M, Tokai.[29] Experimental conditions and methods were as described previously.[15,16]

(27) (a) Takeda, T.; Seto, H.; Komura, S.; Ghosh, S. K.; Nagao, M.; Matsuba, J.; Kobayashi, H; Ebisawa, T.; Tasaki, S.; Zeyen, C. M. E.; Ito, Y; Takahashi, T.; Yoshizawa, H. *J. Phys. Soc. Jpn., Suppl. A* **1996**, *65*, 189. (b) Takeda, T.; Seto, H.; Kawabata, Y.; Okuhara, D.; Krist, T.; Zeyen, C. M. E.; Anderson, I. S.; Hoeghoej, P.; Nagao, M.; Yoshizawa, H.; Komura, S.; Ebisawa, T.; Tasaki, S. *J. Phys. Chem. Sol.* **1999**, *60*, 1599.

(28) Monkenbusch, M.; Schätzler, R.; Richter, D. *Nucl. Instrum. Methods Phys. Res.* **1997**, *A399*, 301.

(29) Ito, Y.; Imai, M.; Takahashi, S. *Physica B* **1995**, *213, 214*, 889.

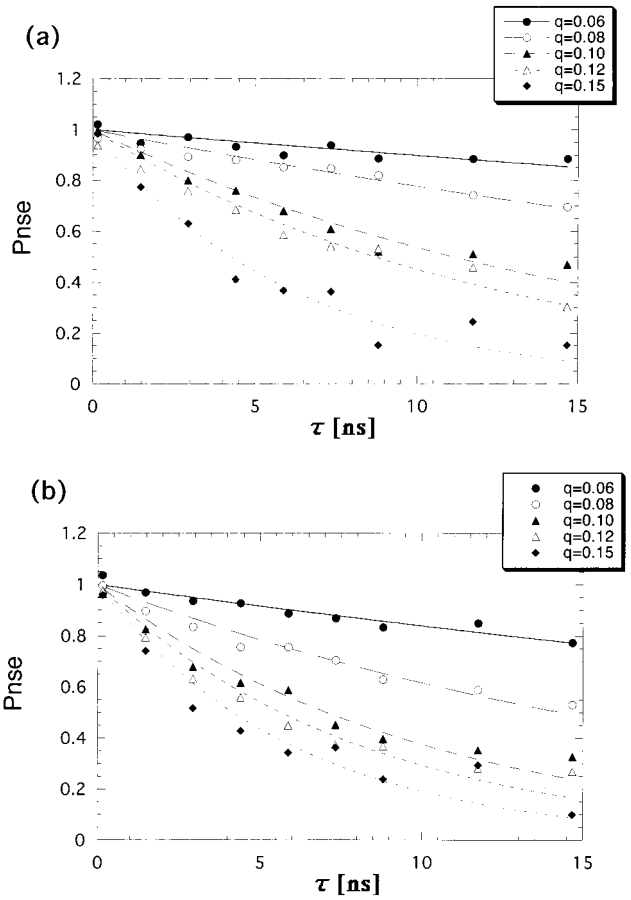

Figure 5. The time correlation function obtained by NSE (P_{nse}) for N496 micelles in 5% D_2O solution at 21 °C (a) and 45 °C (b). The solid and dotted lines show the best-fit curves obtained by single-exponential fitting.

d. DLS Experiments. We performed DLS experiments to estimate the translational diffusion coefficient of polymer micelle independently, using a combination of BI-30 goniometer and BI-9000 correlator (Brookhaven, Ronkonkoma, NY). Details of this instrument and measurement procedures appear elsewhere.[30,31] We also used a D_2O solution to match the experimental condition of NSE. The measurements were performed at scattering angles of 60, 90, and 120 degrees. The obtained time correlation function of scattering intensity was converted to the correlation function for the scattered field $g^{(1)}(q,\tau)$ by utilization of the Siegert relation. The $g^{(1)}(q,\tau)$ functions were analyzed by the cumulant fitting to evaluate the decay rate Γ. To estimate the hydrodynamic radius, we used the Stokes−Einstein equation.

e. SAXS Experiments. We performed the small-angle X-ray scattering (SAXS) experiments to estimate the radius of gyration (R_g) of polymer micelles independently by using an instrument in our laboratory as described elsewhere.[32] The sample cell was a 2-mm ϕ glass capillary (Mark, Germany). The accumulation time was 5000−10 000 s. The scattering from the solvent was measured independently and subtracted from the solution. The data thus obtained were corrected for sensitivity of 1D-PSD (position sensitive detector) and then desmeared.

3. Results and Discussion

a. The Size and Shape of Polymer Micelle. Figures 2a and 2b show the SANS profile for N496 in 1% and 5% D_2O solutions at 21 °C and 45 °C, respectively. At both temperatures, only a slight difference was observed between 1 and 5% in very small angle regions. This can be attributed to the slight intensity decrease by interparticle interference at a higher concentration, 5%. Hence, there was no effect of the concentration in this concentration range. By Guinier analysis[33] for a 1% solution, the $R_{g,Guinier}$ value was estimated to be 49 Å and 48 Å at 21 °C and 45 °C, respectively, that is, unaffected by the temperature in this temperature range. By SAXS measurement, the $R_{g,Guinier}$ value was 58 Å at 25 °C, which is

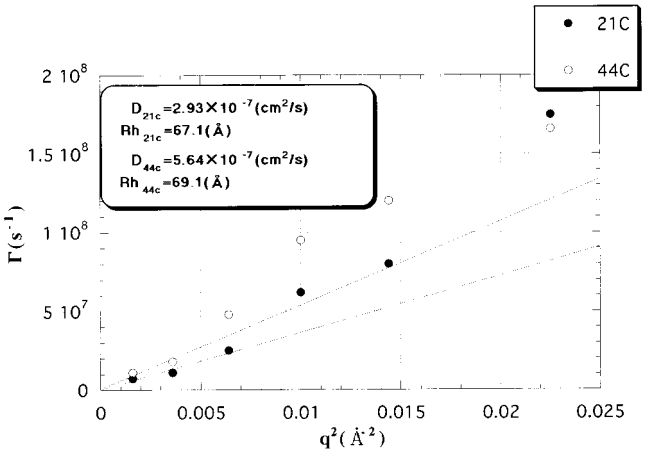

Figure 6. Γ vs q^2 plot for the single-exponential fitting result for N496.

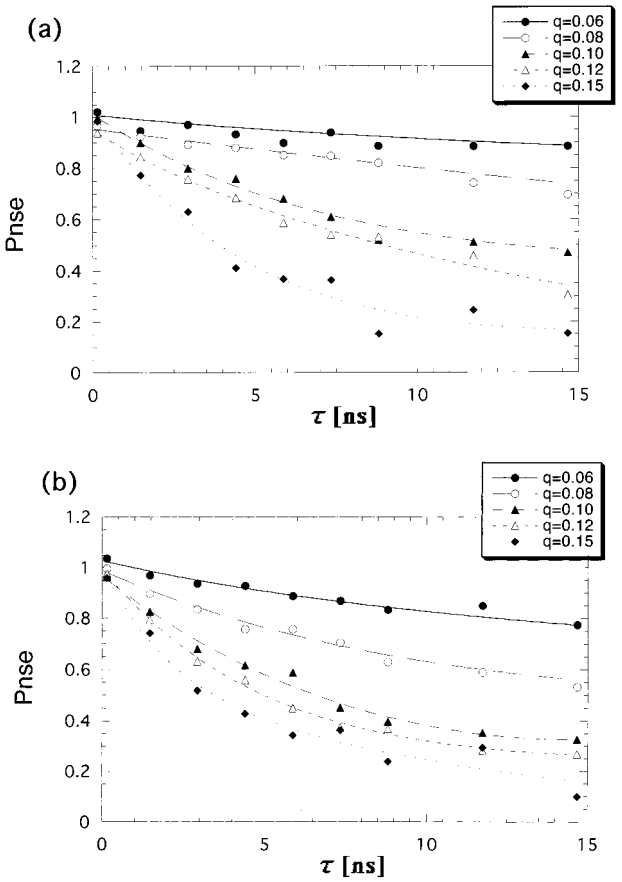

Figure 7. The time correlation function obtained by NSE (P_{nse}) for N496 micelles in 5% D_2O solution at (a) 21 °C and (b) 45 °C. The solid and dotted lines show the best-fit curves obtained by double-exponential fitting.

(30) Matsuoka, H.; Morikawa, H.; Yamaoka, H. *Colloids Surf. A* **1995**, *109*, 137.
(31) Matsuoka, H.; Ogura, Y.; Yamaoka, H. *J. Chem. Phys.* **1998**, *109*, 6125.
(32) Ise, N.; Okubo, T.; Kunugi, S.; Matsuoka, H.; Yamamoto, K.; Ishii, Y. *J. Chem. Phys.* **1984**, *81*, 3294.
(33) Guinier, A.: Fournet, G. *Small-angle Scattering of X-rays*; Wiley: NY, 1955.

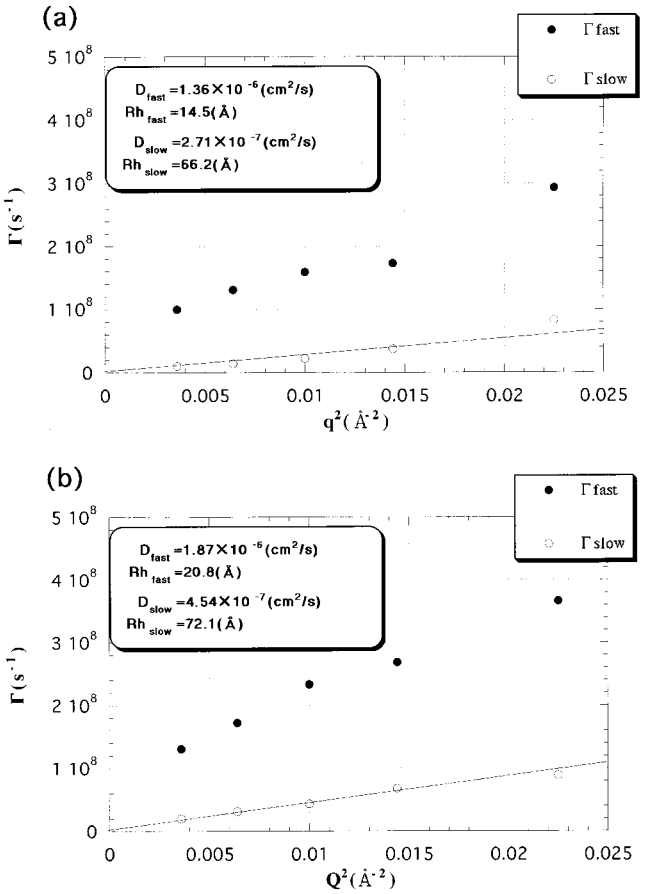

Figure 8. Γ vs q^2 plot for the double-exponential fitting result for N496 at (a) 21 °C and (b) 45 °C.

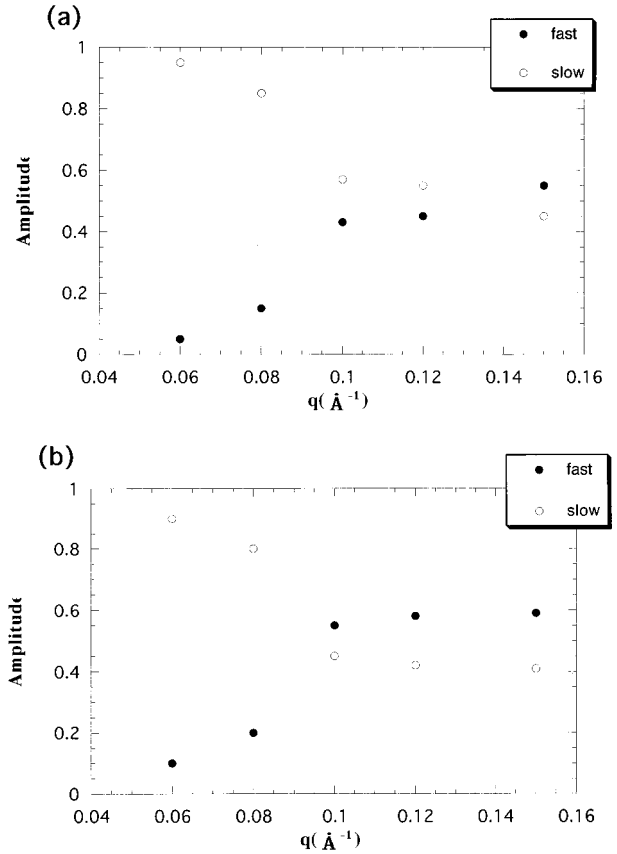

Figure 9. The q dependence of the amplitudes for the fast (A_{fast}) and slow (A_{slow}) modes for N496 at (a) 21 °C and (b) 45 °C.

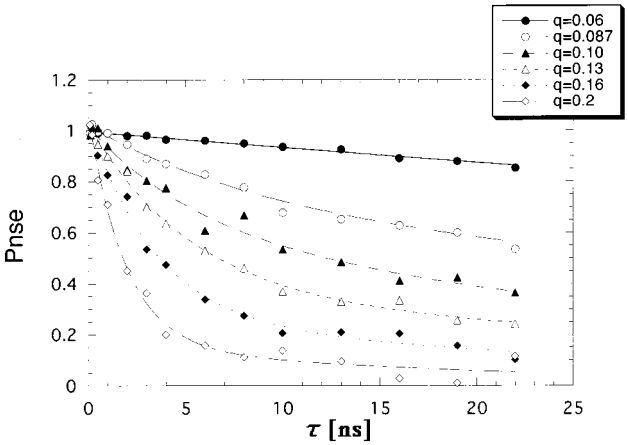

Figure 10. The time correlation function obtained by NSE (P_{nse}) for N338 micelles in a 5% aqueous solution at 25 °C. The solid and dotted lines are the best-fit curves obtained by double-exponential function.

reasonable if the difference of density profiles for electron and scattering length is considered. By the basic scattering theory,[34] for a homogeneous particle, in which the electron/scattering length density is constant, the same R_g value should be obtained by SANS and SAXS. However, in this case the particle is not homogeneous but has a core−shell structure. Hence, the electron density profile is different from the scattering length density profile for the particle, which results in a different $R_{g,Guinier}$ value. Of course, the particle should have its own peculiar R_g value depending on its size and structure, the observation of apparently different $R_{g,Guinier}$ values by SANS and SAXS here means that the particle has inhomogeneous inner structure, i.e., the core−shell structure in this case. NSE experiments were performed at 5% both at 21 °C and 45 °C. The scattering angles, at which NSE experiments were performed, are shown by arrows in Figure 2. Figure 2c shows the SANS profile for N338 micelle in D_2O. Figure 3 shows the model fitting results for both of these micelles. We used the spherical core−shell model and evaluated the core radius (R_c), the whole micelle size (the sum of the core radius and shell thickness), R_s, and the aggregation number (N_{agg}). In this procedure, we used density values of 1.490 and 0.9483 g/cm^3 for HOVE and NBVE, respectively, which were determined in our previous SANS experiments by the contrast variation technique.[15] The results are summarized in Table 1. Reflecting a longer hydrophilic chain (m value) for N496 sample, a smaller N_{agg} value was obtained. The N_{agg} value was calculated from the core volume and volume of a hydrophobic chain with length n. As shown in Figure 3, the core−shell fitting showed a satisfactory agreement with the experimental profile considering the fact that we used a simple core−shell model without polydispersity effect. For N496, R_s = 66 Å was found, whereas $R_{g,Guinier}$ was 49 Å by SANS. For a homogeneous isolated sphere, it is well-known that the relation between R (real sphere radius) and R_g is $R = (5/3)^{1/2}R_g$. By applying this relation to R_g = 49 Å, we find R = 63 Å, which is close to R_s value, 66 Å. This fact may mean that the core−shell nature is not so remarkable for neutrons, different from X-ray case (R_g = 58 Å), which is reasonable and consistent with the difference between the electron density profile (for X-ray) and the scattering length density profile (for neutron). On the other hand,

(34) Higgins, J. S.; Benoit, H. *Polymers and Neutron Scattering*; Oxford, University Press: NY, 1994.

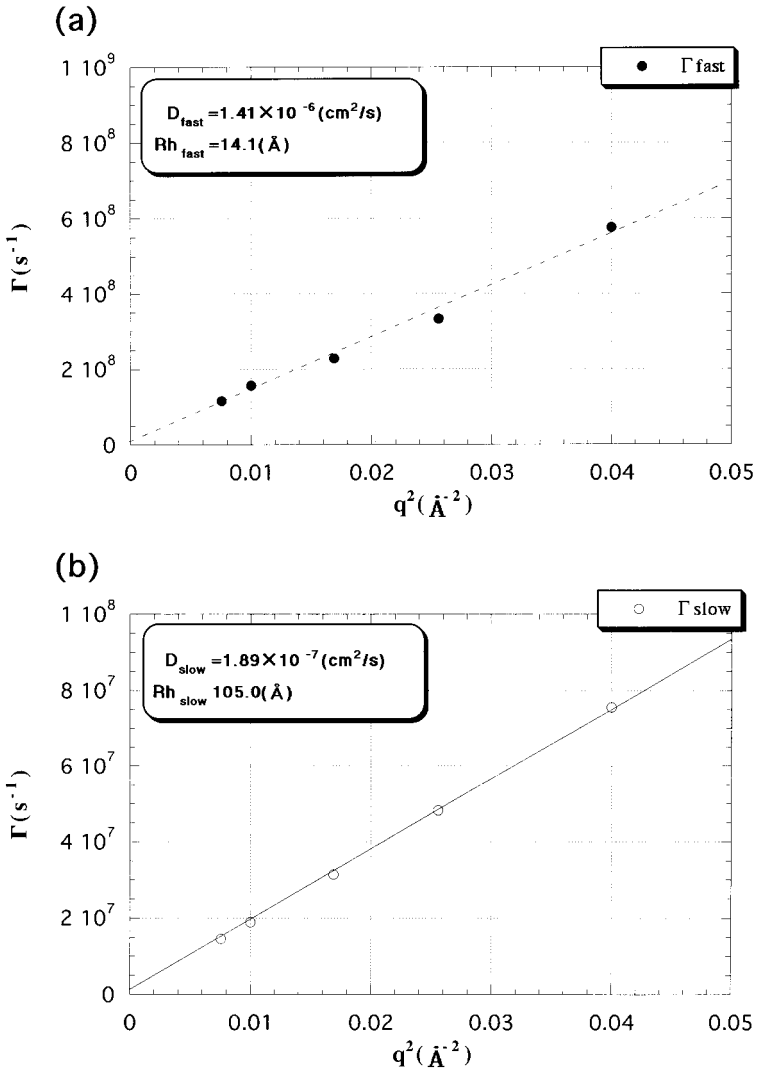

Figure 11. Γ vs q^2 plot for the fast (a) and slow (b) modes for N338.

for the higher q region, a discrepancy was observed in both cases. This has been observed for polymer micelle systems and has been thought to be due to a blob scattering from the micelle shell.[35,36] In the core−shell model, uniform density in the shell was assumed. This is not a bad assumption for a small q region. However, in a higher q region, which reflects a smaller scale structure, SANS detects the scattering from individual polymer chain in the shell. In fact, as shown in Figure 3, the behavior in a higher q region is well described by the Debye function[37] for Gaussian coil. Strictly speaking, it is difficult to believe that the polymer chain with a short length and tethered on the micelle core behaves as an ideal Gaussian coil, but the excellent agreement in Figure 3 means that the main factor in this q region is blob scattering. The obtained $R_{g,Gauss}$ values are reasonable considering the shell thickness and larger value for N496 is consistent with the larger m value.

b. Example of NSE Raw Data. Figure 4 shows a typical example of raw data of an NSE experiment. This is for polymer N496 (5 wt %) at $q = 0.06$ Å^{-1} at 21 °C condition. By fitting the function below,

$$y = M_1 \exp[-C_1(x - M_2)^2]\cos[C_2(x - M_2)] + M_3 \qquad (C_1, C_2; \text{constant})$$

we determined the echo center (M_2) and the amplitude of echo signal ($M_1/M_3(=P_{nse})$).

c. Time Correlation Function for N496. Figure 5 shows the time correlation function obtained by NSE experiments (P_{nse}) for N496 in a 5% D_2O solution at various scattering vectors q. At all angles studied here, this function decayed monotonically with increasing decay time (Fourier time, τ) both at 21 °C and 45 °C. The lines in the figure show the best fit by single-exponential function. The agreement is not unsatisfactory, but for the data with a large q, a distinct disagreement between data and fitting curve can be seen in large F_{time} regions. From this fitting result, the decay rate Γ was calculated by utilization of the following equation;

$$P_{nse}(q,\tau) = \exp(-\Gamma\tau) \qquad (1)$$

If we assume a translational diffusion dynamics, the translational diffusion coefficient D can be calculated from Γ by

$$\Gamma = Dq^2 \qquad (2)$$

This equation predicts that the Γ vs q^2 plot should be a straight line passing through the origin if only a

(35) Richter, D.; Schneiders, D.; Monkenbusch, M.; Willner, L.; Fetters, L. J.; Huang, J. S.; Lin, M.; Mortensen, K.; Farago, B. *Macromolecules* **1997**, *30*, 1053.
(36) Pedersen, J. S.; Gerstenberg, M. C. *Macromolecules* **1996**, *29*, 1363.
(37) Debye, P. *J. Phys. Colloid Chem.* **1947**, *51*, 18.

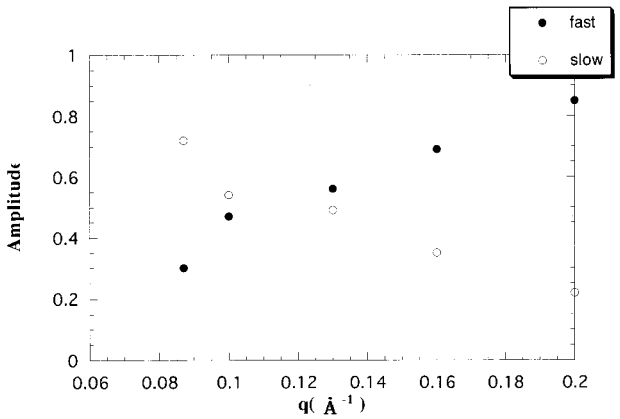

Figure 12. The q dependence of the amplitudes of the fast and slow modes for N338.

translational diffusion dynamics exists and is detected by NSE. This plot is shown in Figure 6. As expected, this plot did not show the excellent straight line passing through the origin. This should be due to the discrepancy at a large τ for large q values. Since the profiles for small q regions were well reproduced by single-exponential fitting, in Figure 6, we tried to draw a straight line from the origin by using only three points at a small q. From its slope, the diffusion coefficient D was evaluated to be 2.93 $\times$ 10^{-7} and 5.64 $\times$ 10^{-7} cm^2/s at 21 °C and 44 °C, respectively. Taking the temperature change of viscosity of the solvent (D_2O) into account, these two diffusion coefficients give us a hydrodynamic radius (R_h) of about 68 Å at both temperatures. The absence of a change in micelle size with temperature is compatible with the SANS result shown in Figure 2. The slightly larger R_h value than R_s is quite reasonable if the hydrodynamic effect is taken into account. A slightly larger R_h value than R_g is reasonable if we consider the relations between the real geometrical size and R_g as described previously.

Because the single-exponential fitting results were not satisfactory, we performed double-exponential fitting using the following function.

$$P_{nse} = A_{fast} \exp(-\Gamma_{fast}\tau) + A_{slow} \exp(-\Gamma_{slow}\tau) \quad (3)$$

Figure 7, a and b shows the results of double-exponential fitting for the data in Figure 5. Obviously, there is a better agreement between the observed profile and fitting curve.

The Γ vs q^2 plots obtained by double-exponential fitting are shown in Figure 8. There was a good linearity for both the fast and slow modes although there was a slight difference in the fast mode for the data with a smaller q value where the contribution of the fast mode was very small (see Figure 9 below). At 21 °C, these slopes gave D_{fast} and D_{slow} values of 1.4 $\times$ 10^{-6} and 2.7 $\times$ 10^{-7} cm^2/s, which correspond to $R_{h\ fast}$ = 15 Å and $R_{h\ slow}$ = 66 Å, respectively, and at 44 °C, D_{fast} and D_{slow} values of 1.9 $\times$ 10^{-6} and 4.8 $\times$ 10^{-7} cm^2/s, which correspond to $R_{h\ fast}$ = 21 Å and $R_{h\ slow}$ = 72 Å, respectively. Although the time correlation functions in Figures 5 and 7 are somewhat scattered, the systematical tendency in Figure 8 indicates the validity of our fitting procedure for these functions.

Figure 9 shows the q dependence of the amplitudes for the fast and slow modes. It is obvious that in smaller q regions the slow mode is dominant, but in larger q regions the fast mode is dominant. At about q = 0.1, the contributions of the two modes are comparable. Thus, the slow mode shows the dynamics for a larger dimension and the fast mode those for a smaller dimension. The systematical tendency in Figure 9 also supports the validity of our analysis here.

Table 2. Comparison of the Diffusion Coefficients of Micelles in D_2O Evaluated by Two Fitting Procedures

polymer	function	D_{fast} ($\times$ 10^{-6} cm^2/s)	D_{slow} ($\times$ 10^{-7} cm^2/s)	
N496	1[a]	1.4	2.7[b]	at 21 °C
	2[c]	1.7	2.6[b]	
	1	1.9	4.5[b]	at 44 °C
	2	2.4	4.5[b]	
N338	1	1.4	1.9[d]	
	2	1.0	2.0[d]	

[a] Function 1: $P_{nse} = A_{fast} \exp(-\Gamma_{fast}\tau) + A_{slow} \exp(-\Gamma_{slow}\tau)$. [b] Obtained by DLS at smallest q and fixed in fitting procedure. [c] Function 2: $P_{nse} = \exp(-\Gamma_{slow}\tau)\{(1 - A_{fast}) + A_{fast} \exp(-\Gamma_{fast}\tau)\}$. [d] Obtained by NSE at smallest q and fixed in fitting procedure.

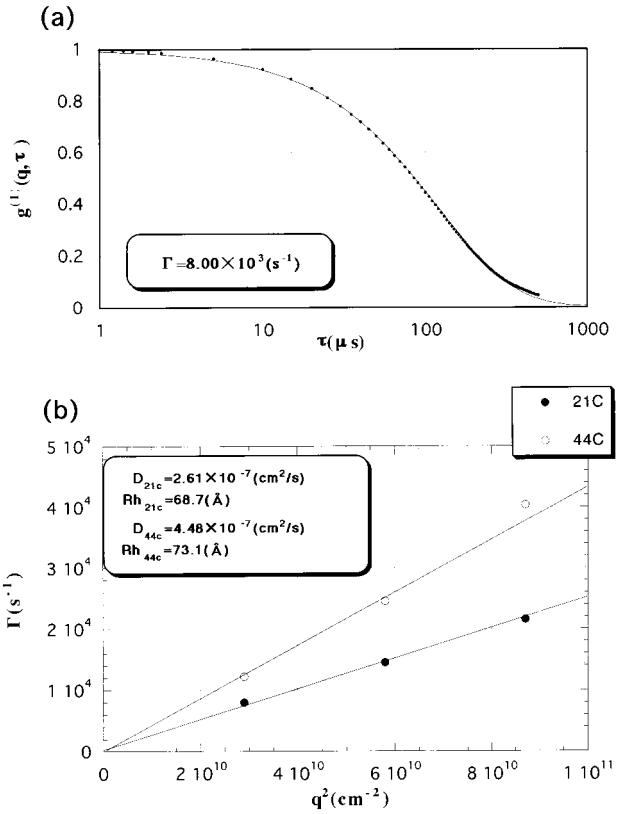

Figure 13. (a) The time correlation function for N496 micelles in aqueous solution (5%) evaluated by DLS. The lines show the best fit by single-exponential fitting at 21 °C, scattering angle of 60°; (b) Γ vs q^2 plot.

d. Time Correlation Function for N338. Figure 10 shows the time correlation function for N338 in a 5% D_2O solution at various q conditions. Because the single exponential fitting did not show satisfactory agreement, as for N496, only the double-exponential fitting results are shown in this figure. The agreement is excellent. The tendency observed for N338 was similar to that for N496. The linearity in Figure 11 is excellent also for the fast mode. In this experiment, the minimum q value was 0.06, which was larger than that for N496, the contribution of the fast mode is already large at this minimum q value. Hence, the data could be fitted with a high accuracy for all q values. Figure 12 shows the q dependence of the amplitudes for the fast and slow modes. As for N496, the fast mode is dominant in higher q regions whereas the slow mode is dominant in lower q regions. The crossover point was also approximately q = 0.11. A similar tendency in Figures 8 and 9 was also observed in Figures 11 and

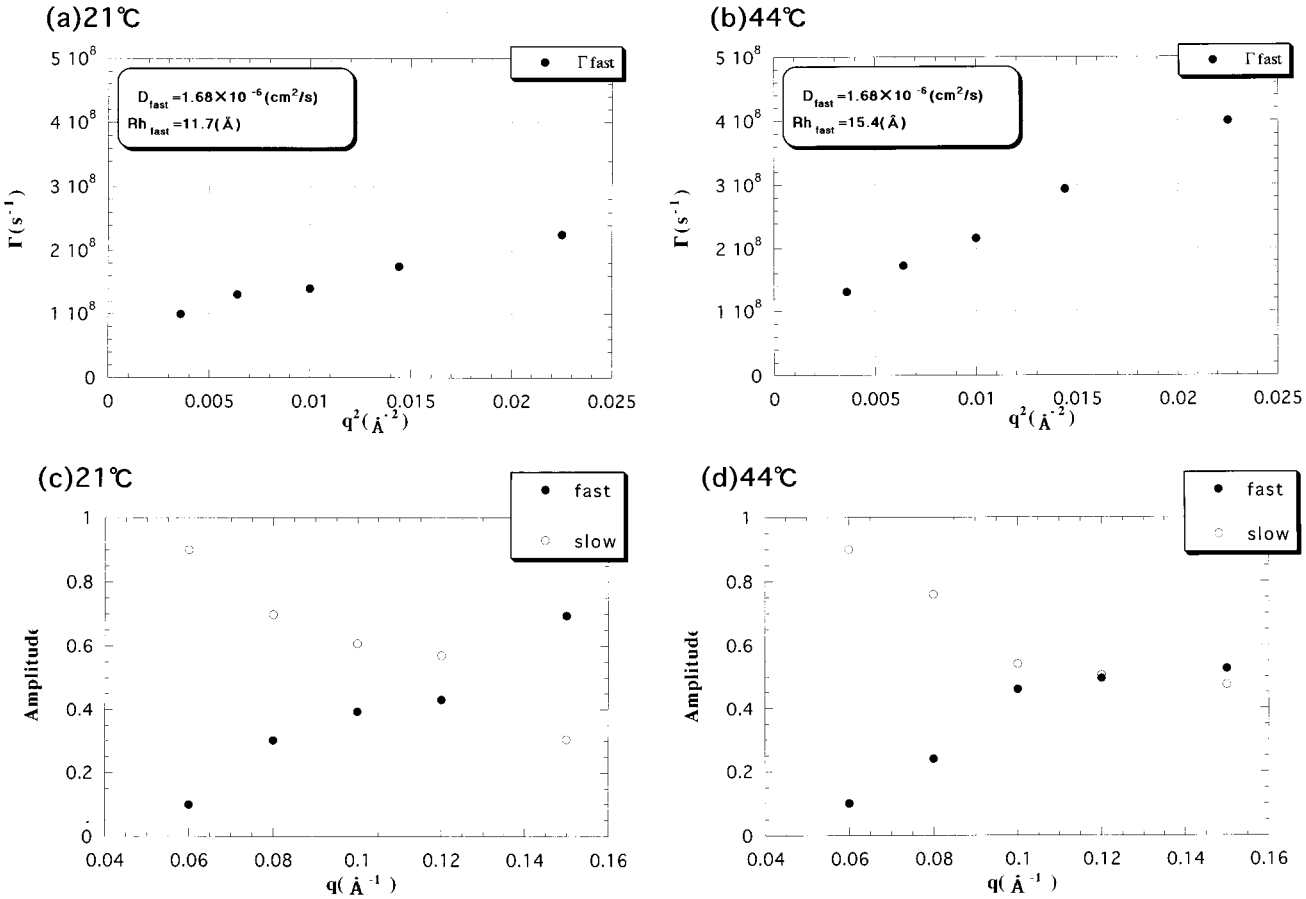

Figure 14. Fitting results of the P_{nse} for N496 by the function $\exp(-\Gamma_{fast}\tau)\{(1-a)+a\exp(-\Gamma_{slow}\tau)$. (a, b) Γ vs q^2 plot for the fast mode, and (c, d) the q dependence of amplitudes for the fast and slow modes. In this fitting, the diffusion coefficient for the slow mode, D_{slow}, was fixed at 2.61×10^{-7} and 4.48×10^{-7} cm^2/s, which were obtained by the DLS measurements.

12 for the N338 sample measured by NSE instrument at Jülich, which supports again the validity of our analysis.

The dynamic modes evaluated by NSE for these two polymer micelles are summarized in Table 2.

e. The Origin of the Fast and Slow Modes. The q positions of NSE experiments are shown by the arrows in Figures 2 and 3. Measurement was not possible in smaller q regions because of the effect of the direct beam and in larger q regions because of insufficient scattering intensity. The SANS profiles imply that the angular range for the NSE experiment lays on the border of the so-called Guinier regions[33] and Porod region.[38] Hence, it is reasonable to assume that the dynamic behavior both for the whole micelle and internal structure can be detected at the same time in these q ranges. From the comparison between R_h values by NSE and micelle size estimated by SANS and SAXS, the slow mode, D_{slow} and $R_{h\ slow}$, should be for the translational diffusion of the polymer micelle itself. To confirm the validity of this conclusion, we performed DLS experiments for the N496 sample. The results (time correlation function) are shown in Figure 13. This time correlation function was well reproduced by cumulant fitting, and the slope of Γ vs q^2 plot gave us R_h values of 68 Å and 73 Å at 21 °C and 44 °C, respectively, which are in excellent agreement with the NSE value for the slow mode ($R_{h,slow}$ = 66 Å by NSE at 21 °C). It is reasonable that DLS can detect only the translational diffusion of the micelle (slow mode in NSE) because DLS covers only a very small q range that corresponds to the fluctuation of large dimensions; the dynamics in a small scale, such as the internal motion of a polymer micelle, cannot be observed by DLS. Hence, the slow mode in NSE data corresponds to the translational diffusion of the whole micelle.

Figures 9 and 12 clearly show that the amplitude, that is, the contribution, of the slow mode decreased with increasing q, whereas, that of the fast mode increased. This tendency also supports our conclusion above for the origin of the fast and slow modes. With increasing q, the scattering detects the structure and fluctuation of a smaller dimension.

At this moment, we cannot justify the linearity of the fast mode shown in Figures 8 and 11. If this is an internal dynamic mode in the polymer micelle, this mode is not translational dynamics. Hence, in these plots the fast mode need not give a straight line passing through the origin. Frankly speaking, the excellent linearity observed in Figure 11 was unexpected. The most suitable explanation for the origin of the fast mode might be the "corona" dynamics of the polymer micelle. As mentioned in the introduction, several investigators have drawn this conclusion for the nonaqueous system. Some theoretical approaches have also been taken.[26] One possible factor might be the existence of unimers in the system. As in the low molecular weight micellar system, also in the polymer micelle system there are unimers with a concentration equal to the critical micelle concentration (cmc). Because unimers show translational diffusion, there is a possibility that NSE detected this motion of unimers. However, the concentration of unimers should be very low. Our polymers have a cmc value of about 0.02 wt %; lower by 2 orders of magnitude. In addition, by the basic scattering theory,

(38) Porod, G. *Kolloid.-Z.* **1951**, *124*, 83.

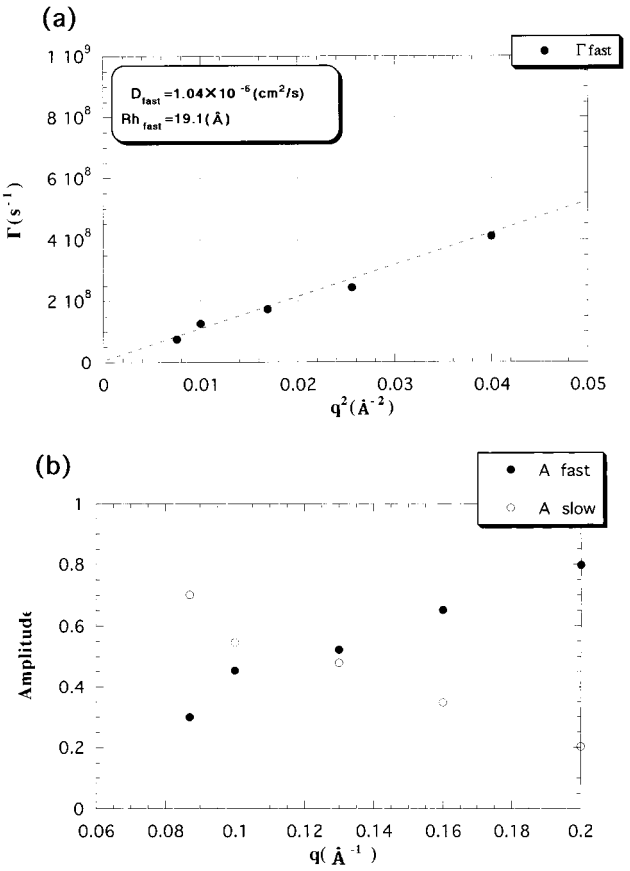

Figure 15. Fitting results of the P_{nse} for N338 by the function $\exp(-\Gamma_{fast}\tau)\{(1-a)+a\exp(-\Gamma_{slow}\tau)\}$. (a) Γ vs q^2 plot for the fast mode, and (b) the q dependence of amplitudes for the fast and slow modes. In this fitting, the diffusion coefficient for the slow mode, D_{slow}, was fixed at 2.03×10^{-7} cm^2/s, which was obtained from the NSE data at the lowest q value.

the scattering intensity proportional to the square of the volume of the scatterer.[33,34] Hence, the scattering intensity from unimers is expected to be very weak and not a significant contributor to the NSE data here. However, this possibility should be examined in more detail in the future because the linearity in Figure 11a is excellent.

f. Further Analysis of P_{nse}. For the analysis of time correlation function, such as $g^{(1)}_{(q,\tau)}$ by DLS and P_{nse} by NSE, single-exponential fitting and the double-exponential fitting are common and useful techniques. In fact, we have performed the double-exponential analysis above. However, according to our conclusion above, that is, the slow mode is the translational diffusion of the whole polymer micelle in water and the fast mode is the internal model for the hairy corona (shell) of the polymer micelle, might be more appropriate to use the following functions as a fitting function for analysis,

$$P_{nse} = \exp(-\Gamma_{slow}\tau)\{(1 - A_{fast}) + A_{fast}\exp(-\Gamma_{fast}\tau)\} \quad (4)$$

where $A_{slow} = 1 - A_{fast}$. This concept comes from the idea that the internal corona mode is not independent of the translational diffusion of the whole polymer micelle: the hairy corona, which shows the internal fast motion, is fixed on the polymer micelle which is moving at a decay rate of Γ_{slow}. Hence the fast mode is "convoluted" to the slow mode and one of its model functions is eq 4. We fitted P_{nse} by eq 4 with fixed D_{slow} values, hence Γ_{slow}: one value is that obtained by NSE at the smallest q value, which might reflect only the slow mode, and the other is that obtained by DLS. The former method was applied to N338 data and the latter to N496 data. The results are shown in Figures 14 and 15. Although almost no significant improvement can be found for N486, slightly "better" linearity in the Γ vs q^2 plot is observed for N338. A similar q dependence of the amplitude was also detected. There seems to be no serious difference in the choice of D_{slow} value. The diffusion coefficients obtained by this method and the double-exponential method are summarized in Table 2.

Although we believe that the origin of the fast mode is the corona dynamics, more detailed analysis is necessary to clarify this point completely. Further analysis for time correlation function, such as fitting by stretched exponential, is one possibility. A careful estimation of the dependence of Γ on q is also an important factor. A theoretical approach, such as that which Monkenbusch et al. applied,[26] might be also interesting because it has not been applied and tested for aqueous systems.

4. Conclusions

By systematic NSE experiments, we found the presence of two dynamic modes, the fast and the slow modes, for amphiphilic diblock copolymer micelles in aqueous solutions. At smaller q values, the slow mode was the dominant, whereas at larger q values, the fast mode was dominant. The diffusion coefficient D for the slow mode of the N496 sample was about 2.7×10^{-7}cm^2/s at 21 °C, which gave a hydrodynamic radius of about 70 Å. Because SANS, SAXS, and DLS gave almost the same geometrical size, this slow mode is considered to be the translational motion of the whole micelle. At 44 °C, the slow mode in NSE gave the same size of micelle, which is in good agreement with the results obtained by SANS and DLS. Similar results were obtained for the N338 sample. The fast mode, which is faster than the slow mode by 1 order of magnitude, is thought to be the dynamic mode of the hydrophilic shell (corona). More detailed analyses, such as a comparison with theoretical prediction, is now underway. Here, we demonstrated that NSE is a very powerful tool to study dynamics that cannot be covered by the DLS technique for spatial dimension and time order.

Acknowledgment. This work was financially supported by grants-in-aid for Scientific Research by the Ministry of Education, Sports, and Culture of Japan (A09305062 and 00086208) to whom our sincere gratitude is due. The measurements at Jülich were supported by a Grant for Joint Research Project under the Japanese-German Cooperative Science Promotion Program from both Japan Society for Promotion of Science and Deutsche Forschungsgemeinschaft. NSE experiments at Tokai was accepted as Proposal No. 98-104. H.M., M.N., and H.E. would like to express their sincere thanks to the members of Institut für Festkorperforschngs for their kind support during their stay at Jülich and especially for R.Schäzler for his kind technical assistance in the NSE measurements at Jülich.

LA9915421